ACS Sustainable Chemistry & Engineering

Research Article

pubs.acs.org/journal/ascecg

Preparation of Microfibrillated Cellulose Composites for Sustained Release of H_2O_2 or O_2 for Biomedical Applications

Chia-Wen Chang and Meng-Jiy Wang*

Department of Chemical Engineering, National Taiwan University of Science and Technology, 43 Keelung Rd., Sec. 4, Taipei 106, Taiwan

Supporting Information

ABSTRACT: A cost-effective and energy-saving approach to prepare microfibrillated cellulose (MFC) nanocomposites from natural wood fibers is reported. The MFC was mixed with calcium peroxide (CPO) with or without catalase to form multilayered MFC nanocomposites that allow modulation of the releases of hydrogen peroxide (H_2O_2) or oxygen (O_2), respectively. The release profile of H_2O_2 from the MFC nanocomposites up to five days was obtained, and the effects of H_2O_2 and O_2 on the responses of mammalian cells were evaluated. The results showed that MFC itself possesses great biocompatibility, and the MFC/CPO nanocomposites are able to suppress cell proliferation. The further addition of catalase into the MFC/CPO composites converts H_2O_2 to O_2 so effectively that enhanced L-929 fibroblasts cell density was clearly found. The as-prepared MFC/CPO and [MFC+catalase]/CPO nanocomposites were shown to be applicable on alternative substrates and revealed similar functions. Moreover, the cell cultured on the [MFC+catalase]/CPO composites under a serum-free condition revealed that the generation of oxygen plays a role in supporting cell proliferation. This study is among the first work to report the modulation of the release of H_2O_2 and O_2 by using microfibril cellulose-based materials for applications in wound sterilization and to accelerate wound healing.

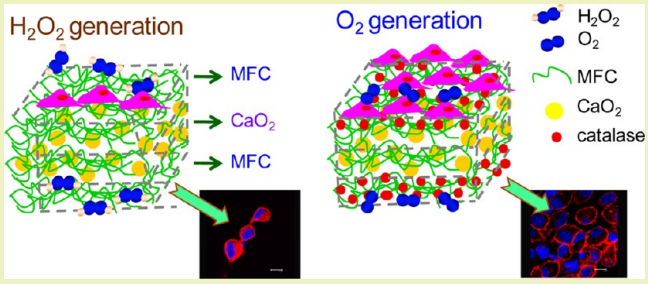

KEYWORDS: *Catalase, Hydrogen peroxide, Microfibrillated cellulose (MFC), Oxygenation, Scaffold*

INTRODUCTION

The utilizations of recycled or wasted materials for value-added applications such as biodiesel and biomedical materials have attracted tremendous attention in recent years due to the increased costs of new materials and the shortage of natural resources. Microfibrillated cellulose (MFC) was applied to various fields due to its nanostructure, great biocompatibility, and excellent mechanical property.

Tissue engineering scaffolds fabricated by biomimetic approaches such as extracellular matrix (ECM)-like environments and porous structures revealed particular incentives for the promotion of affinities between biomolecules and materials.[1] Various techniques were employed to prepare biomimetic scaffolds by creating topological niches[2] or providing biological functionalities.[3] In particular, biomaterials with porous structures offer a three-dimensional microenvironment and showed improved cell affinity when compared with flat surfaces.[4,5] Natural polymers such as chitosan,[6] collagen,[7] and cellulose[8] revealed versatility for applications in biomaterials, and an increasing number of works were devoted to create porous scaffolds from the aforementioned materials.[9−11]

Herrick et al. and Turbak et al. reported the preparattion of microfibrillated cellulose (MFC) by homogenizing the dilute slurries of wood cellulose pulp repetitively under high pressure.[12] The average diameter of MFC fibers are 1−50 nm and several micrometers in length. Therefore, MFC is regarded as fiber with nanostructure.[13] MFC possesses advantageous properties including large surface area due to its nanoscaled and interconnected fibrils, outstanding mechanical property, biodegradability, and biocompatibility.[14] Moreover, the sources of naturally abundant wood pulps and the characteristic of easy processing expand the wider applicability for MFC.

Hydrogen peroxide is the simplest peroxide that was often employed as a cleaning agent and oxidizing agent. In physiological condition, most human cells are exposed to certain level of hydrogen peroxide. Nevertheless, the cytotoxicity becomes an issue for tissue survival when the concentration of H_2O_2 exceeds 50 mM.[15] H_2O_2 also plays a role in antibacterial applications for wound dressing, biocide, and for tooth bleaching.[16,17] The most commonly used methods for preparing H_2O_2 such as hydrogenation, filtration, and extraction, are usually complex and require multiple steps of manufacturing. The concentration of oxygen in physiological condition is crucial for promoting tissue repair and regeneration.[18] For example, the establishment of in vivo vascularization for implanted organs relies on the supplies of oxygen and nutrients from blood. In addition, the lack of oxygen supply might also cause myocardial infarction, which is

Received: February 20, 2013
Revised: May 29, 2013
Published: June 12, 2013

dx.doi.org/10.1021/sc400054v | ACS Sustainable Chem. Eng. 2013, 1, 1129−1134

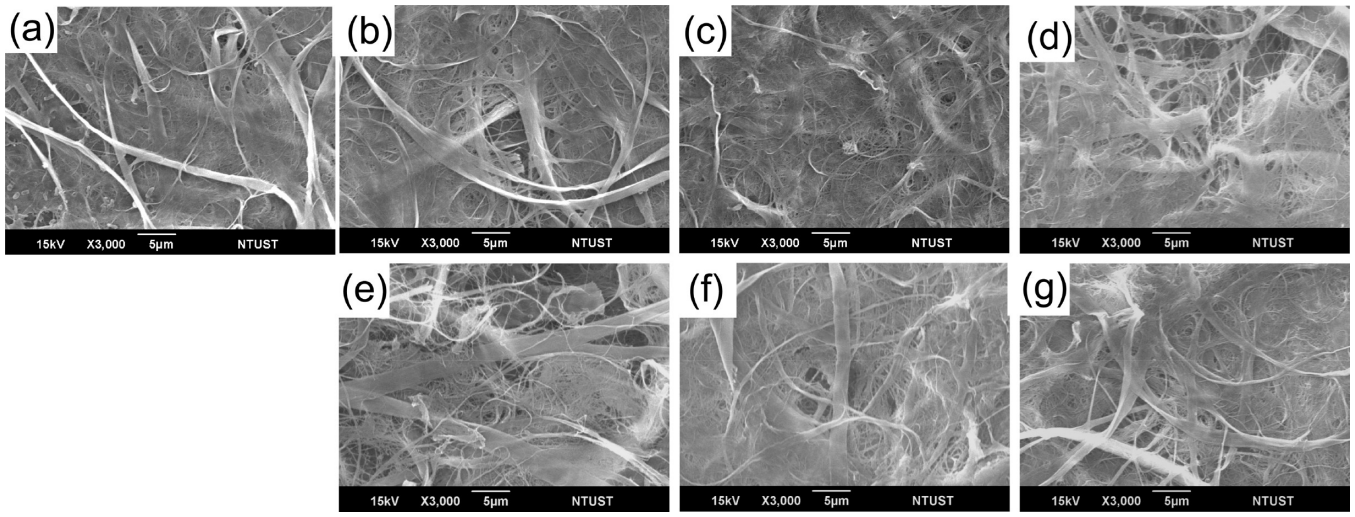

Figure 1. Surface morphology on (a) pristine MFC. MFC/CPO with different CPO concentrations: (b) 5, (c) 10, and (d) 15 wt %. MFC/[CPO +catalase] with different CPO concentrations: (e) 5, (f) 10, and (g) 15 wt %.

a serious cardiac disease.[19] Synthetic biomaterials, usually lacking oxygen generating functions, are not suitable for long-term clinical applications because of tissue damage or cell death under hypoxic conditions. It is therefore important to develop materials that are able to self-generate oxygen or to provide a platform for the supplies of gas and nutrients diffusion.

In this study, a cost-effective method using materials originated from natural wood pulps is proposed to prepare sandwiched MFC composites that control the release of H_2O_2 or O_2 and further modulate the growth of mammalian cells. Calcium peroxide (CPO) that reacts with water to release H_2O_2 under physiological condition was embedded in two layers of MFCs to form MFC/CPO. The further addition of catalase, a natural enzyme existing in living tissue, into MFC/CPO to form [MFC+catalase]/CPO allowed for the conversion of H_2O_2 to oxygen sustainably under room temperature with a fast reaction rate. The release rate of H_2O_2 was monitored for five days, meanwhile the effects of cytotoxicity and tissue regeneration were evaluated by cultivating L-929 mouse fibroblasts on the MFC/CPO and [MFC+catalase]/CPO. Moreover, the as-prepared MFCs were also integrated onto a polydimethylsiloxane (PDMS) substrate to demonstrate the utility of the MFC nanocomposites. To the best of our knowledge, this study is among the first work to report the potential of modulating the release of H_2O_2 and O_2 using wood fibers and a solvent-free process without consuming much solvents and energy. The developed versatile microfibrillated cellulose membranes provide promising in vivo generation of H_2O_2 or oxygen generation for antimicrobial, wound dressing, and tissue regeneration applications.

EXPERIMENTAL SECTION

Materials. All chemicals were purchased from Sigma unless specified otherwise. The crude microfibrillated cellulose (MFC), brick-like microfibril cellulose, and calcium peroxide (CaO_2, CPO) were purchased from Daicel Chemical Industries Ltd. (Japan) and Acros Organics, respectively. All materials were used without further purification. Catalase and p-benzoquinone were purchased from Sigma-Aldrich. Rhodamine-conjugated phalloidin was acquired from Molecular Probes, U.S.A. (R415). DAPI was purchased from Chemicon International, Inc., U.S.A. (S7113). Analytical grade chemical and reagents used for preparation of calcium peroxide composite membrane were used as received.

Preparation of MFC Nanocomposites. Crude MFC was first homogenized in DI water at high speed for 40 min and then underwent centrifugation through gradient of ethanol solutions (from 30 to 99 wt %) to remove water. The concentration of MFC was 1 wt % in pure ethanol. The composite was prepared in a layer-by-layer manner, where the MFC/CPO-*x* was composed of MFC, a mixture of MFC and CPO-*x*, and MFC, where *x* represents the weight percentage of CPO (x = 5, 10, 15, respectively). The thickness of the prepared MFC nanocomposites was shown in Figure S1 of the Supporting Information. Moreover, [MFC+catalase]/CPO-*x* was prepared by three layers of MFC+catalase, MFC and CPO-*x*, and MFC+catalase.

Surface Characterizations. Surface morphology of the MFC membrane was observed by scanning electron microscope (JEOL JSM-6300). The chemical composition was evaluated by electron spectroscopy for chemical analysis (ESCA). Thermo VG Scientific Theta Probe Instrument with a monochromatic source of Al Kα (1486.6 eV) as excitation source was operated with pass energy of 50 eV. An Ar ion gun was employed with 3 kV voltage and 1 mA current.

Measurements of H_2O_2 Release. The release of H_2O_2 was carried out at a closed batch system for five days. A total of 0.5 mg/mL p-benzoquinone aqueous solution was prepared and poured into each closed tube. MFC/CPO with different CPO concentrations was immersed in the tube to measure the amount of released H_2O_2. H_2O_2 tends to self-decompose easily to two electrons, two protons, and one oxygen molecule in solution. p-Benzoquinone was employed as a mediator to react with the generated H_2O_2 and form hydroquinone, as shown in eqs 1 and 2.

$$H_2O_2 \leftrightarrow 2H^+ + 2e^- + O_2 \quad (1)$$

$$\text{p-benzoquinone} + 2H^+ + 2e^- \leftrightarrow \text{hydroquinone} \quad (2)$$

The reaction is accompanied with the color change and can be measured under ultraviolet spectrometer at the wavelength of 360 nm. The UV spectrum for the absorption of p-benzoquinone and hydroquinone is shown in Figure S2a of the Supporting Information, and the obtained calibration curve for the concentration of H_2O_2 is shown in Figure S2b of the Supporting Information. It is assumed that the same reaction rate for the production of H_2O_2 and least reversible reaction was considered.

Cell Culture. Cell culture of L-929 fibroblasts was performed in a humidified incubator with 5% CO_2 at 37 °C. All culture media were purchased from Sigma: Dulbecco's modified eagle medium (DMEM-high glucose); trypsin, lyophilized powder; EDTA; fetal bovine serum; sodium bicarbonate; sodium pyruvate; and L-glutamine. The L-929 cells were cultivated on the MFC samples from 24 h to five days, and

the cell culture medium was changed every three days. The initial cell seeding density was 20,000 cells/mL.

Cell Viability Assay. The density of the viable cells was determined by performing lactate dehydrogenase (LDH) assay as previously reported. The attached cells were lysed with 250 μL of 1% Triton X-100 in PBS. The reaction solution contained 1/12 NAD+, 1/12 diaphorase, 1/12 bovine serum albumin, 1/12 sucrose, 1/3 iodonitrotetrazolium, and 1/3 sodium lactate. The optical density values were read at 490 nm by using enzyme-linked immunosorbent assay (ELISA, iMark Absorbance Reader, BioRad). The cell density was calculated based on the prepared calibration curve obtained by using sequentially diluted cell solutions.

L-929 fibroblasts were fixed on the surface of composites by immersing in a solution of 4% paraformaldehyde in phosphate buffered saline (PBS, pH 7.4) and followed by permeabilized with 0.1% Triton X-100 at room temperature. The actin filaments and nuclei of cells were stained with 165 nM of rhodamine-conjugated phalloidin and DAPI (1:1000 dilutions) for 20 min at room temperature. Confocal laser scanning microscopy (CLSM) was utilized to visualize the stained cells (Leica-SP2, Germany)

Statistic Analyses. Variations of all data were statistically analyzed by performing one-way analysis of variance (ANOVA), executed by origin lab software. To compare the statistical difference of each sample, the asterisk mark (*) was applied as * for p-value <0.05, ** for p-value <0.01, and *** for p-value <0.001.

RESULTS AND DISCUSSION

The prepared MFC nanocomposites were characterized by scanning electron microscopy (SEM) and ESCA. The cell-material interactions were investigated by directly cultivating L-929 fibroblast cells on the MFCs.

Surface Morphology of MFC Nanocomposites. The surface morphology of pristine MFC was visualized by SEM, which revealed the highly porous structure of MFC with twisted fibers (Figure 1a). The fibers with submicrometer diameter and pores facilitated the mass transportation and gas diffusion through the microstructure to the peripheral environment of the membranes. Similar surface morphology was observed on all MFC/CPO-x and [MFC+catalase]/CPO-x with different concentrations of CPO, indicating that the incorporation of CPO and catalase did not show impact on the pore size and surface morphology of membranes (Figures 1b–g). Moreover, no small particle was observed from the SEM images, confirming the well embedment of CPO and catalase in the nanocomposites.

Chemical Compositions for MFC Nnocomposites. Table 1 summarizes the surface chemical composition of pristine MFC, MFC/CPO, and [MFC+catalase]/CPO analyzed by elemental surface chemistry analysis (ESCA). Carbon and oxygen are the most important two elements on all MFCs that the atomic carbon content is 64.6% on pristine MFC and decreased slightly after the incorporation of CPO to about ~60% on MFC/CPO-x and ~57% on [MFC+catalase]/CPO-x. On the other hand, the oxygen content increased slightly from ~40% to 43% on [MFC+catalase]/CPO when compared with that on MFC/CPO which is presumably resulted from the oxygen functional groups of catalase. Moreover, it is noted that no calcium signal was found on ESCA wide scan spectra, confirming again the well entrapment of CPO in MFCs.

Table 1. Chemical Composition on Different MFC Membranes

	sample	element (atom %)			
		C_{1s}	O_{1s}	N_{1s}	Ca_{2p}
pristine MFC		64.6	35.4	–	–
wt % of CPO	MFC/CPO-5	60.7	39.3	–	–
	MFC/CPO-10	59.2	40.4	–	–
	MFC/CPO-15	61.1	38.9	–	–
	[MFC+catalase]/CPO-5	57.0	43.0	–	–
	[MFC+catalase]/CPO-10	57.2	42.7	0.1	–
	[MFC+catalase]/CPO-15	56.7	43.2	–	–

H_2O_2 Release Profile. H_2O_2 was released as soon as water molecules penetrated into the middle layer (MFC+CPO-x) of the composite membranes, and then the generated H_2O_2 diffused out of the membranes gradually via the pores. The release behavior was monitored for one week. Figure 2a revealed that an initial burst release of H_2O_2 was observed on all MFC/CPO-x for the first few hours, followed by a steady-state release after 24 h. The amount of released H_2O_2 depended on the quantity of embedded CPO. The maximum concentration of released H_2O_2 was 327, 167, and 69 mM on MFC/CPO-15, MFC/CPO-10, and MFC/CPO-5, respectively.

Cell Responses on MFCs. L-929 fibroblast was directly cultivated on all MFC composites to investigate the effects of released H_2O_2 and O_2 for a short period (one day) and long-term (five days) that correspond to the release duration of H_2O_2. It is noted that the commonly used cell culture plate TCPS (tissue culture polystyrene) is used as a control group to compare with the normal cell growth rate. On TCPS, cell density was ~20,000 cells/cm^2 at day 1 and increased to ~34,200 cells/cm^2 at day 5 (Figure 2b).

On pristine MFC, L-929 fibroblasts grew linearly, from ~4500 to 38,900 cells/cm^2 on the pristine MFC from day 1 to day 5. It is noted that the cell density on the pristine MFC was even higher than that on TCPS at day 5, presumably due to the highly porous MFC that provides the microenvironment niches for cell growth. The results showed that pristine MFC is a material with excellent biocompatibility.

MFC/CPO-x composites showed the toxicity due to the generation of H_2O_2 and that the cell density was ~3200, 2800 and 3000 cells/cm^2 on MFC/CPO-5, MFC/CPO-10, and MFC/CPO-15 after 24 h of cell culture. At day 5, the number of cells increased slowly to 5100, 5300 and 8400 cells/cm^2 on MFC/CPO-5, MFC/CPO-10, and MFC/CPO-15, respectively, which is much lower than that on the pristine MFCs (<21%).

The results confirmed that the sustained release of H_2O_2 during five days caused cell apoptosis. The death of cells was presumably due to the toxicity from H_2O_2 and the hydroxyl radicals (HO•), which were decomposed from H_2O_2.[20] It is also noted that the concentration of CPO did not have a significant influence on the cell density, indicating that 5% of CPO is sufficient for the generation of H_2O_2 and hydroxyl radicals (HO•) for the extent of toxicity to result in cell death.

On the other hand, the number of cells increased on all [MFC+catalase]/CPO-x composites. Cell density was ~3400, 2900, and 3300 cells/cm^2 at day 1 and increased to ~6500 cells/cm^2, 6200 cells/cm^2, and 32,400 cells/cm^2 at day 5 on [MFC+catalase]/CPO-5, [MFC+catalase]/CPO-10, and [MFC+catalase]/CPO-15, respectively (Figure 2b). It was observed that at day 5 a similar cell density was found on [MFC +catalase]/CPO-5 and [MFC+catalase]/CPO-10 but increased to more than 9 fold on [MFC+catalase]/CPO-15, which is even comparable with the cell density on TCPS, indicating sufficient oxygen supplies for cell growth. The results implied

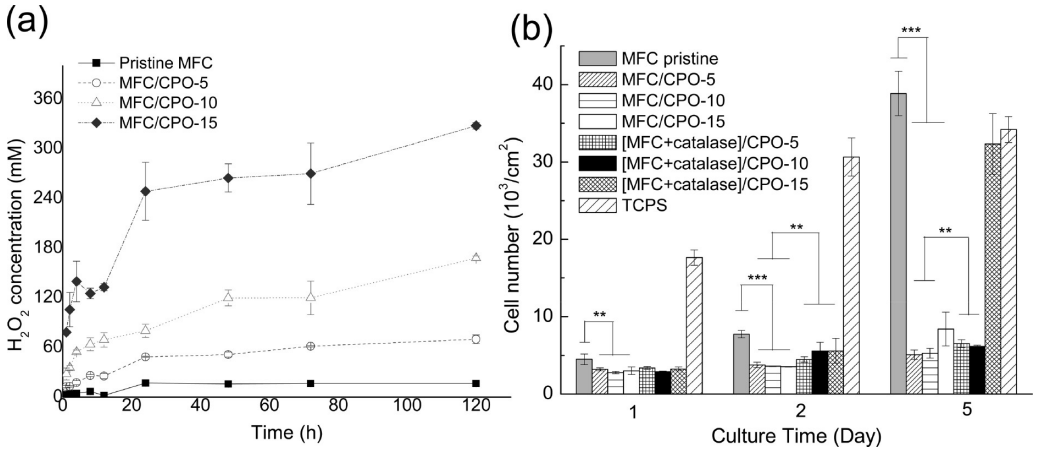

Figure 2. (a) Release profile of H_2O_2 on MFC/CPO for 120 h. (b) Cell viability on pristine MFC, MFC/CPO, and [MFC+catalse]/CPO. Cell density was evaluated by LDH assay and measured at 1, 2, and 5 days; $N = 5$; ** and *** represent $p < 0.01$ and $p < 0.001$, respectively).

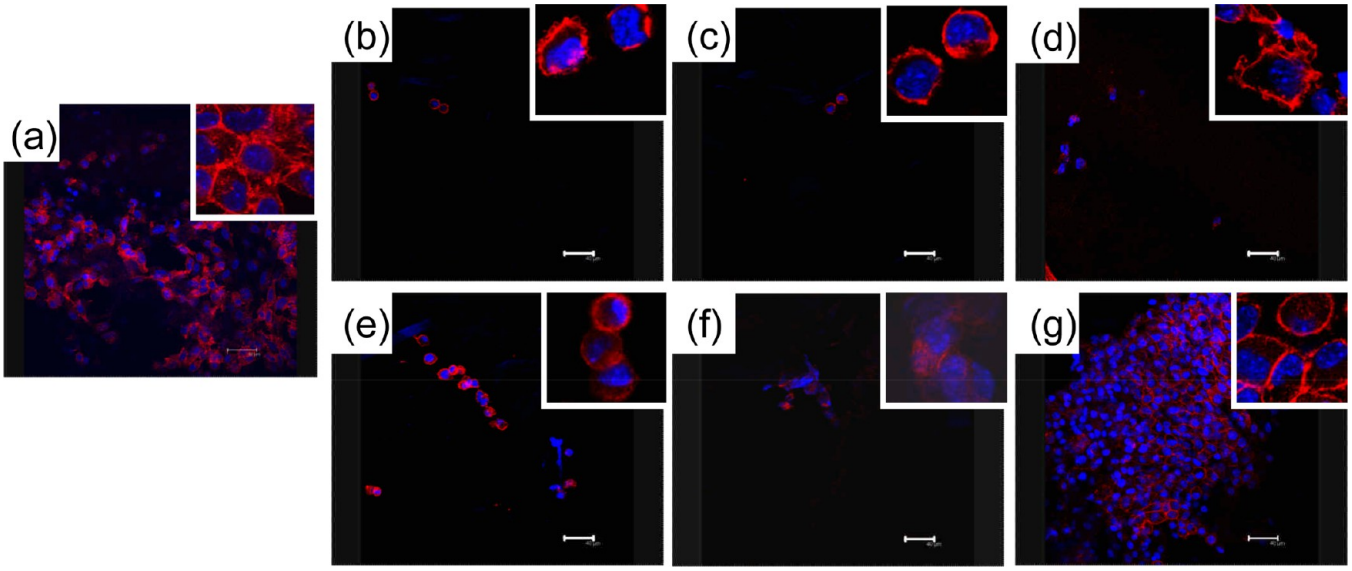

Figure 3. Cell morphology on (a) pristine MFC. MFC/CPO-*x* with different CPO concentration: (b) 5, (c) 10, and (d) 15 wt %. MFC/[CPO +catalase] with different CPO concentration: (e) 5, (f) 10, and (g) 15 wt %. Scale bar = 40 μm.

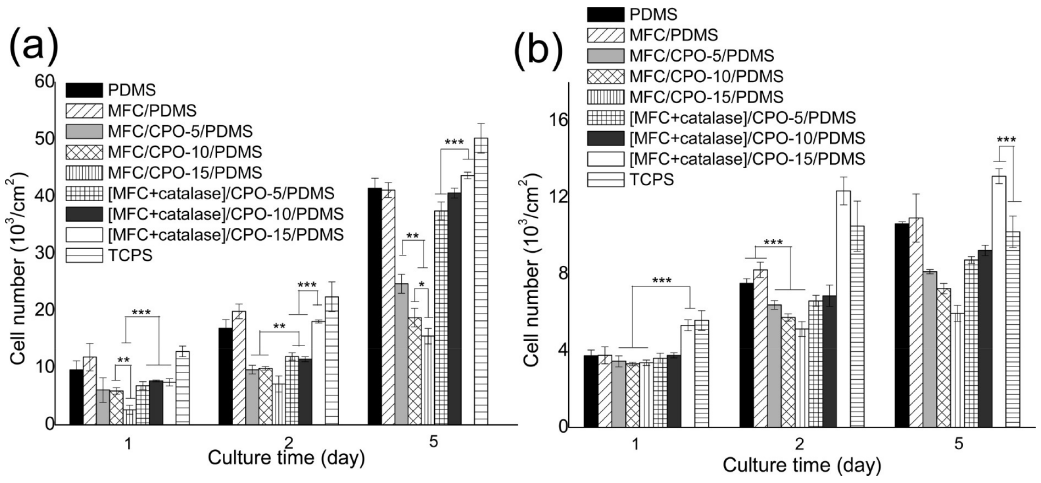

Figure 4. Cell density on MFC/PDMS, MFC/CPO-*x*/PDMS, and [MFC+catalase]/CPO-*x*/PDMS composites (a) under serum-containing condition and (b) under serum-free condition. Cell density was evaluated by LDH assay and measured at 1, 2, and 5 days; $N = 3$; *, **, and *** represent $p < 0.05$, $p < 0.01$, and $p < 0.001$, respectively.

dx.doi.org/10.1021/sc400054v | *ACS Sustainable Chem. Eng.* 2013, 1, 1129−1134

that the incorporation of catalase catalyzed the conversion of H_2O_2 to O_2 effectively, which provided oxygen for cell proliferation. Moreover, the particularly high cell density on [MFC+catalase]/CPO-15 might be due to the highly porous structure of MFC, which provided extremely large surface area. Less significant impact on cell density for short period (day 1) was presumably due to the time period required for cells to adapt to the vicinity. In addition, less significant impacts were received by cells for shorter cell culture period (one day), presumably because most of the cells were adapting to the vicinity during the first few hours.

In addition to cell density, cell morphology on all MFC composites was observed by confocal laser scanning microscope (CLSM) after seven days of cell culture. Figure 3 revealed that the number of cells reached confluence after seven days on pristine MFC, which is in consistent with the cell viability results, as well as an indication of the cell viability of a long culture period. In contrast, only a limited number of cells was found on all MFC/CPO-*x*. Moreover, more cells were found on [MFC+catalase]/CPO-5 and [MFC+catalase]/CPO-10 when compared to that on the MFC/CPO-*x* (Figures 3b–f). Furthermore, a high cell density was found on [MFC +catalase]/CPO-15, confirming the results obtained from cell viability (Figure 3g).

Cell Responses on MFC Composite-Coated PDMS. The prepared MFC nanocomposites were also applicable on different substrates. In this study, the MFCs were integrated on polydimethylsiloxane (PDMS), which is often used as substrates for microfluidic channels and biochips. L-929 fibroblasts were cultured on pristine-MFC/PDMS, MFC/CPO-*x*/PDMS, and [MFC+catalase]/CPO-*x*/PDMS to investigate cell responses when H_2O_2 or O_2 was released. Furthermore, the fibroblasts were cultivated in both serum-containing and serum-free conditions to evaluate the importance of the supplies of oxygen and nutrients (serum) on cell behavior.

The cell number of L-929 increased linearly on pristine PDMS and is comparable than that on pristine MFC and TCPS under the serum-containing condition. (Figure 4a). Similarly, the generation of H_2O_2 resulted in the decrease in cell viability on MFC/CPO-*x*/PDMS that ~6100, 6000, and 2600 cells/cm^2 were found on MFC/CPO-5/PDMS, MFC/CPO-10/PDMS, and MFC/CPO-15/PDMS at day 1 and increased to 24,700, 18,800, and 15,600 cells/cm^2 at day 5, respectively. The cell number on MFC/CPO-15/PDMS decreased significantly, so that the ratio of cell density compared to that on pristine MFC was 22%, 36%, and 38% at day 1, day 2, and day 5, respectively.

The incorporation of [MFC+ catalase]/CPO-*x* on PDMS also revealed the successful conversion of H_2O_2 to O_2, which led to higher cell viability. The cell density was similar at day 1 on [MFC+catalase]/CPO-5/PDMS, [MFC+catalase]/CPO-10/PDMS, and [MFC+catalase]/CPO-15/PDMS (~7000–7500 cells/cm^2). On the other hand, the number of L-929 fibroblasts increased 1.49 fold and 2.43 fold at day 2 on [MFC +catalase]/CPO-5/PDMS and [MFC+catalase]/CPO-10/PDMS, respectively, and further enhanced to about 3 fold at day 5. Notably, cell density on [MFC+catalase]/CPO-15/PDMS (~ 43,600 cells/cm^2) at day 5 showed a comparable cell number in comparison with that on TCPS (~50,200 cells/cm^2). The responses of L-929 fibroblasts showed similar results on MFCs/PDMS with that directly cultivated on MFCs, which indicate the potential application of applying MFC composites on biomedical devices such as microfluidic biochips and related devices.

For the samples cultured in serum-free condition, for 24 h, the cell number on PDMS, pristine MFC, and all MFC/CPO-*x*/PDMS did not show apparent differences, so that the cell density is ~3,300 cells/cm^2 (Figure 4b). The cell number increased slightly on [MFC+catalase]/CPO-5/PDMS and [MFC+catalase]/CPO-10/PDMS, so that the cell density was ~3700 cells/cm^2. It is noted that the cell density on [MFC +catalase]/CPO-15/PDMS (~5300 cells/cm^2) is comparable with that on TCPS (~5600 cells/cm^2) at day 1, indicating the excellent biocompatibility of [MFC+catalase]/CPO-15. The reason that L-929 fibroblasts grew even better on TCPS under the serum-free condition is because that the commercially available TCPS is usually modified with a coating layer of protein or with plasmas. The results also indicated that serum plays a very essential role for modulating the initial cell attachment and cell growth.

More significant impacts from the release of H_2O_2 and O_2 were found at day 2, so that the cell density was ~6400, 5700, and 5100 cells/cm^2 on MFC/CPO-5/PDMS, MFC/CPO-10/PDMS, and MFC/CPO-15/PDMS, respectively. On the other hand, the cell density increased to ~6600, 6900, and 12,300 cells/cm^2 on [MFC+catalase]/CPO-5/PDMS, [MFC+catalase]/CPO-10/PDMS, and [MFC+catalase]/CPO-15/PDMS, respectively. It is noted that the cell density on [MFC +catalase]/CPO-15/PDMS was even higher (~12,300 cells/cm^2) than that on TCPS (~10,500 cells/cm^2).

Cell density increased slightly at day 5, which might be due to the limited nutrients in medium. Nevertheless, the cell density of ~13,100 cells/cm^2 was found on [MFC+catalase]/CPO-15/PDMS, which was significantly higher than that on TCPS (~10,200 cells/cm^2). Moreover, the cell density on MFC/CPO-5/PDMS, MFC/CPO-10/PDMS, and MFC/CPO-15/PDMS was 25.7%, 34.7%, and 46.6% lower than that on the pristine MFC/PDMS, respectively, indicating the cytotoxicity of H_2O_2. These results suggest the potential usage for the supplies of oxygen by coating [MFC+catalase]/CPO on biomedical devices in limited nutrients surroundings.

The cell morphology under the serum-free culture condition was revealed by optical microscope. Limited cell quantity was observed on pristine MFC and all MFC/CPO-*x*/PDMS (Figure S3, Supporting Information). Nevertheless, an increased cell number on [MFC+catalase]/CPO-*x*/PDMS was easily found when compared to that on MFC/CPO-*x*/PDMS, indicating that oxygen provides nutrients in some extent to promote cell proliferation. In conclusion, both L-929 cell responses on MFC composite-decorated PDMS with or without serum suggest that an approach for modulating cell responses on different substrates for biomedical engineering and clinical purposes.

4. CONCLUSION

Highly porous and biomimetic nanocomposites that allow for modulating the growth of L-929 fibroblasts were prepared by incorporating calcium peroxide (CaO_2) and catalase into microfibrillated cellulose using a facile and solvent-free approach. CaO_2 was employed to produce hydrogen peroxide, while catalase was added to catalyze the conversion of H_2O_2 to O_2. The experimental results showed that the three-dimensional porous morphology facilitated both the diffusion of generated gases and provided great niches for cell growth. Sustained release of H_2O_2 up to five days was found on the

prepared MFC nanocomposites. Cell attachment decreased, and cell proliferation was clearly delayed due to the generation of H_2O_2 on MFC/CPO. On the other hand, cell survival was effectively promoted on the MFC containing CPO and catalase. The as-prepared MFC nanocomposites were also applicable on other substrates and demonstrated the same effects on cell responses. Further works on culturing cells on the prepared MFC nanocomposites under a serum-free condition indicated that generation of oxygen support effectively aided the cell growth when no serum was provided. In conclusion, the prepared MFC/CPO nanocomposites that allow the release of H_2O_2 are aimed to be applied in the fields of wound dressing, tooth bleaching, and antimicrobial applications. On the other hand, the [MFC+catalase]/CPO composites that release O_2 possess particular potentials for applications in tissue regeneration and research on stem cells.

■ ASSOCIATED CONTENT

Supporting Information

Thickness of prepared MFC nanocomposites, how released H_2O_2 was measured, and cell morphology on MFC/CPO-x/PDMS and [MFC+catalase]/CPO-x/PDMS. This material is available free of charge via the Internet at http://pubs.acs.org.

■ AUTHOR INFORMATION

Corresponding Author

*Tel: +886-2-2730-1146. Fax: +886- 2-2737-6644. E-mail: mjwang@mail.ntust.edu.tw.

Notes

The authors declare no competing financial interest.

■ ACKNOWLEDGMENTS

The authors express special appreciation to the National Science Council (99-2221-E-011-121-MY2) in Taiwan for their financial supports.

■ REFERENCES

(1) Liu, X.; Smith, L. A.; Hu, J.; Ma, P. X. Biomimetic nanofibrous gelatin/apatite composite scaffolds for bone tissue engineering. *Biomaterials* **2009**, *30*, 2252−2258.

(2) Chen, W.; Villa-Diaz, L. G.; Sun, Y.; Weng, S.; Kim, J. K.; Lam, R. H. W. Nanotopography influences adhesion, spreading, and self-renewal of human embryonic stem cells. *ACS Nano* **2012**, *6*, 4094−4103.

(3) Ho, Q. P.; Wang, S. L.; Wang, M. J. Creation of biofunctionalized micropatterns on poly(methyl methacrylate) by single-step phase separation method. *ACS Appl. Mater. Interfaces* **2011**, *3*, 4496−4503.

(4) Zhang, X.; Reagan, M. R.; Kaplan, D. L. Electrospun silk biomaterial scaffolds or regenerative medicine. *Adv. Drug Delivery Rev.* **2009**, *61*, 988−1006.

(5) Karageorgiou, V.; Kaplan, D. Porosity of 3D biomaterial scaffolds and osteogenesis. *Biomaterials* **2005**, *26*, 5474−5491.

(6) Dash, M.; Chiellini, F.; Ottenbrite, R. M.; Chiellini, E. Chitosan—A versatile semi-synthetic polymer in biomedical applications. *Prog. Polym. Sci.* **2011**, *36*, 981−1014.

(7) Miyata, T.; Taira, T.; Noishiki, Y. Collagen engineering for biomaterial use. *Clin. Mater.* **1992**, *9*, 139−148.

(8) Bodin, A.; Bäckdahl, H.; Petersen, N.; Gatenholm, P. Bacterial Cellulose as Biomaterial. In *Comprehensive Biomaterials*; Ducheyne, P., Ed.; Elsevier: Amsterdam, The Netherlands, **2011**; pp 405−410.

(9) Yamaguchi, I.; Itoh, S.; Suzuki, M.; Sakane, M.; Osaka, A.; Tanaka, J. The chitosan prepared from crab tendon. I: The characterization and the mechanical properties. *Biomaterials* **2003**, *24*, 2031−2036.

(10) Chen, Z. G.; Wang, P. W.; Wei, B.; Mo, X. M.; Cui, F. Z. Electrospun collagen−chitosan nanofiber: A biomimetic extracellular matrix for endothelial cell and smooth muscle cell. *Acta Biomater.* **2010**, *6*, 372−382.

(11) Ku, S. H.; Park, C. B. Human endothelial cell growth on mussel-inspired nanofiber scaffold for vascular tissue engineering. *Biomaterials* **2010**, *31*, 9431−9437.

(12) Herrick, F. W.; Casebier, R. L.; Hamilton, J. K.; Sandberg, K. R. Microfibrillated cellulose: Morphology and accessibility. *J. Appl. Polym. Sci.* **1983**, *37*, 797−813.

(13) Stenstad, P.; Andresen, M.; Tanem, B.; Stenius, P. Chemical surface modifications of microfibrillated cellulose. *Cellulose* **2008**, *15*, 35−45.

(14) Lavoine, N.; Desloges, I.; Dufresne, A.; Bras, J. Microfibrillated cellulose—Its barrier properties and applications in cellulosic materials: A review. *Carbohydr. Polym.* **2012**, *90*, 735−764.

(15) Bladier, C.; Wolvetang, E. J.; Hutchinson, P.; Haan, J. B. d.; Kola, I. Response of a primary human fibroblast cell line to H_2O_2: Senescence-like growth arrest or apoptosis? *Cell Growth Differ.* **1997**, *8*, 589−598.

(16) Naik, S.; Tredwin, C. J.; Scully, C. Hydrogen peroxide tooth-whitening (bleaching): Review of safety in relation to possible carcinogenesis. *Oral Oncol.* **2006**, *42*, 668−674.

(17) Smith, T. J.; Kennedy, J. E.; Higginbotham, C. L. The rheological and thermal characteristics of freeze-thawed hydrogels containing hydrogen peroxide for potential wound healing applications. *J. Mech. Behav. Biomed. Mater.* **2009**, *2*, 264−271.

(18) Harrison, B. S.; Eberli, D.; Lee, S. J.; Atala, A.; Yoo, J. J. Oxygen producing biomaterials for tissue regeneration. *Biomaterials* **2007**, *28*, 4628−4634.

(19) Roger, V. L.; Go, A. S.; Lloyd-Jones, D. M.; Adams, R. J.; et al. Heart disease and stroke statistics—2009 Update. A report from the American Heart Association Statistics Committee and Stroke Statistics Subcommittee. *Circulation* **2011**, *123*, e18−e209.

(20) D'Autréaux, B.; Toledano, M. B. ROS as signalling molecules: Mechanisms that generate specificity in ROS homeostasis. *Nat. Rev. Mol. Cell Biol.* **2007**, *8*, 813−824.